Chemical Engineering Journal 522 (2025) 167254

Contents lists available at ScienceDirect

Chemical Engineering Journal

journal homepage: www.elsevier.com/locate/cej

Electrochemical anaerobic fluidized bed membrane bioreactor: Sustainable management of membrane fouling and enhancement of methane production rate in greywater treatment

Minseok Kim [a], Dayoung Ko [b], Minyeong Lee [a], Changsoo Lee [b,c], Jeonghwan Kim [a,*]

[a] Department of Environmental Engineering, Program of Environmental and Polymer Engineering, Inha University, Inharo-100, Michuhol-gu, Incheon, Republic of Korea
[b] Department of Civil, Urban, Earth, and Environmental Engineering, Ulsan National Institute of Science and Technology (UNIST), Ulsan 44919, Republic of Korea
[c] Graduate School of Carbon Neutrality, Ulsan National Institute of Science and Technology (UNIST), Ulsan 44919, Republic of Korea

ARTICLE INFO

Keywords:
Electrochemical anaerobic fluidized bed membrane bioreactor
Greywater
Antifouling
Methane production
Extracellular electron transfer

ABSTRACT

A novel electrochemical anaerobic fluidized bed membrane bioreactor (E-AFMBR) was developed and applied to enhance both methane production kinetics and antifouling efficiency from synthetic greywater treatment. A unique feature of the E-AFMBR is the integration of electrochemical interactions, driven by external voltage, with mechanical scouring actions caused by media fluidization across the ceramic membrane surface to ensure sustainable operation. Compared to the control AFMBR (C-AFMBR) operated under the same organic loading rate (OLR) without external voltage, the E-AFMBR produced 48.9 % more biomethane at an applied voltage of −1.00 V. Furthermore, antifouling efficiency in the E-AFMBR was 50 % higher than that in the C-AFMBR. These synergistic effects were more pronounced at longer hydraulic retention times (HRTs) or lower set-point permeate fluxes. The electrical energy produced by biomethane was about 50 % higher in the E-AFMBR than in the C-AFMBR. Microbial community analysis revealed that hydrogenotrophic *Methanobacterium* and electroactive *Geobacter* were more dominant in the E-AFMBR than in the C-AFMBR. The findings of this study strongly support the E-AFMBR as one of the most promising anaerobic membrane bioreactor (AnMBR) technologies for achieving energy-positive, decentralized wastewater treatment and resource recovery by enhancing both antifouling efficiency and methane production rate.

1. Introduction

Anaerobic membrane bioreactors (AnMBRs) have gained attention as a promising approach for treating wastewater while simultaneously obtaining renewable energy in the form of biomethane from wastewaters [1,2]. These systems allow independent control of solid retention time (SRT) and hydraulic retention time (HRT), making them well-suited for decentralized wastewater treatment and resource recovery applications requiring compact footprints [3–5]. However, membrane fouling, which is caused by the accumulation of contaminants on the membrane surface and within its pores, remains a key operational challenge [6,7]. Fouling leads to reduced membrane permeability and can ultimately compromise the long-term stability and performance of AnMBR systems.

Anaerobic fluidized bed membrane bioreactor (AFMBR) integrates membrane filtration with a fluidized biocarrier, offering a distinctive approach to reduce membrane fouling at very low energy demand typically less than 0.1 kWh/m^3 [8–11]. A key advantage of the AFMBR is that the biocarriers, such as granular activated carbon (GAC) particles, are fluidized along the membrane surface by bulk recirculation through the reactor, enabling mechanical scouring to retard foulant accumulation on the membrane. This configuration can eliminate the need for biogas sparging which is energy-intensive to reduce the membrane fouling [9–11]. In a previous study, for example, Alsam et al. [9] reported that when using the GAC with a specific gravity of 2.2 at a 50 % (*v*/v) of packing ratio based on reactor volume, the energy consumption for the GAC fluidization was only 0.023 kWh/m^3. Similarly, Kim et al. [11] found that the energy consumption required to operate an AFMBR added with polyvinylidene fluoride (PVDF) media as a biocarrier was 0.0144 kWh/m^3. Furthermore, Kim et al. [10] reported that the energy consumption for fluidizing spherical polyethylene terephthalate (PET) beads as scouring agent in an AFMBR (50 % packing ratio) was 0.022

* Corresponding author.
E-mail address: jeonghwankim@inha.ac.kr (J. Kim).

https://doi.org/10.1016/j.cej.2025.167254
Received 22 May 2025; Received in revised form 12 August 2025; Accepted 14 August 2025
Available online 14 August 2025

kWh/m^3. In addition, the biocarriers applied into AFMBR provide a large surface area for biofilm formation, thereby contributing to the maintenance of high microbial concentrations for methane production [12,13]. As a result, these combined effects create a synergistic impact not only on fouling control but also on bioenergy production in wastewater treatment.

In spite of many advantages of AFMBR, the use of fluidized biocarriers themselves may not be sufficient to mitigate internal membrane fouling, which is primarily caused by pore blockage and adsorption of soluble microbial products (SMPs) [14]. Such fouling is associated with small colloidal substances which can be penetrated through membrane pores, leading to increase membrane resistance against hydraulic flows [15,16]. In addition, the methane production rate employed by low-strength wastewater such as greywater is still very slow through the AFMBRs, although high biomass can be retained by biocarriers. Furthermore, as biocarriers are broken during operational period, biofilm formed on them should be disrupted, and thus eventually leading to system failure [17].

Integrating electrochemical technology with AFMBR is a promising way because it has high synergistic impacts on the enhancement of methane production kinetics and antifouling efficiency [18,19]. Applying an external voltage creates electrostatic repulsion between charged foulants and the membrane surface, thereby reducing membrane fouling through electrostatic interactions [20–22]. Additionally, electric fields can facilitate electron transfer between microbial species. Previous studies showed that the use of conductive carbon nanotube (CNT) hollow-fiber membranes as cathodes in an anaerobic electrochemical MBR (AnEMBR) controlled both membrane fouling and methane production kinetics effectively [23]. Moreover, electric fields can be helpful to prevent the formation of complexes between organic matter and divalent cations, which may otherwise contribute to pore blockage [24]. When operating AnEMBR with CNT hollow-fibers, transmembrane pressure (TMP) was −0.35 bar at 8 h HRT and −1.2 V external voltage. This value was significantly lower than that obtained from the same reactor operated under the same HRT (−0.6 bar) but without external voltage [25]. Despite these beneficial impacts, technical limitations still need to be overcome to increase permeability of CNT membranes, and standardize protocols regarding fouling control strategies such as backwashing, relaxation, or chemical cleaning [18,23,26–28].

To address the limitations mentioned above, this study combined external voltage with media fluidization into AFMBR to enhance the system performance from synthetic greywater treatment. To improve system stability, a ceramic membrane with high permeability and a polymer-based fluidized media with superior mechanical strength were further applied into the electrochemical AFMBR (E-AFMBR). Unlike previous two-stage microbial electrolysis cell (MEC)-AFMBR configurations [29,30], the E-AFMBR system developed in this study was applied as a single-stage reactor, enabling compact reactor design. This unique feature can make the E-AFMBR particularly suitable for decentralized wastewater treatment and resource recovery, where small footprint is required.

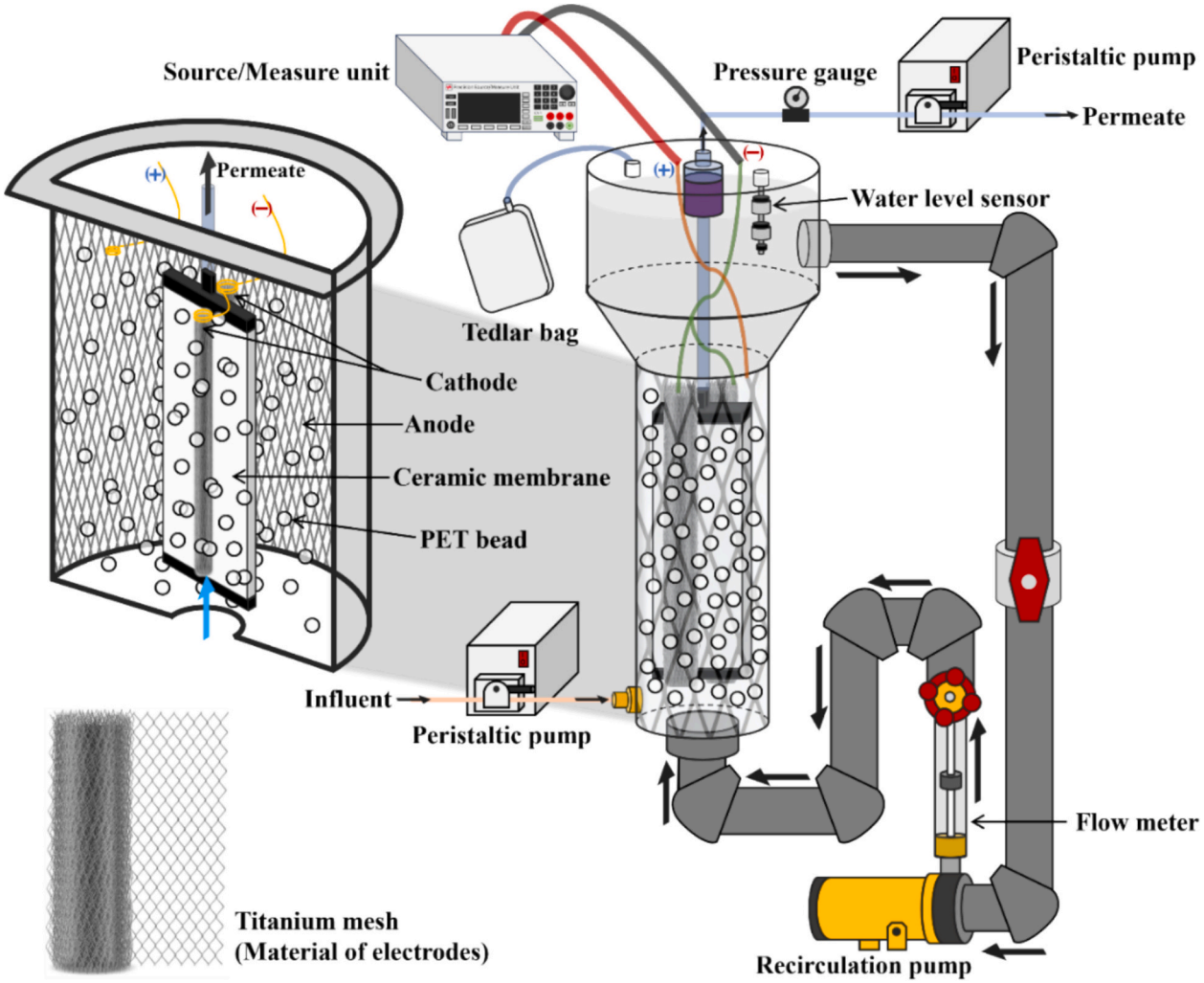

Fig. 1. Schematic diagram of E-AFMBR.

The main objective of this study was to investigate the combined effects of external voltage and fluidized media in the E-AFMBR on membrane fouling, methane production rate, and microbial communities in synthetic greywater treatment. The long-term performance of the E-AFMBR was compared with that of a control AFMBR (C-AFMBR) operated in parallel without external voltage under identical varying HRT (or set-point flux) conditions.

2. Materials and methods

2.1. E-AFMBR set-up

A schematic diagram of a laboratory-scale E-AFMBR system operated in this study is shown in Fig. 1. A cylindrical reactor was made of acrylic with 4.1 L of effective reactor volume. A magnetic-drive centrifugal pump (NH-50PX, PAN WORLD, Japan) was installed in a recycle line (Fig. 1) to drive upward flow of the bulk suspension through the reactor. PET beads with a diameter of 2–3 mm were used as fluidized media, and 800 mL of the beads were added into the E-AFMBR. The PET beads were fluidized along the membrane surface by recirculating bulk flow through the reactor at 18 L/min to cover the whole membrane surface area. Throughout the long-term AFMBR operation, the PET beads were expected to retain their physical and chemical stability, thereby maintaining consistent and effective fluidization status. The PET beads used in our study have excellent mechanical properties, with tensile strength of 50–75 MPa and Young's Modulus of 2.0–2.8 GPa. The density of PET beads with approximately 1.38 g/cm^3 enabled stable fluidization under bulk recirculation through the reactor. These physical properties ensure high structural integrity and resistance against deformation during long-term reactor operations. The PET beads are also known for high chemical resistance. As a result, under anaerobic conditions, the PET beads can be fluidized without their physical degradation during our long-term operational period. A flat-tubular ceramic membrane (Meidensha Corporation, Japan) was vertically submerged into the reactor. Effective surface area and nominal pore size of the membrane were 0.052 m^2 and 0.1 μm, respectively. A titanium electrode, made by titanium mesh was installed and positioned around both sides of membrane surfaces as the cathode. The titanium cathode chamber was filled by 40 g of GAC, accounting for 1.95 % of the total effective reactor volume (4.1 L). The GAC particles used in the reactor had a Brunauer-Emmett-Teller (BET) area of 673.51 m^2/g, thus providing a large porous area for biofilm formation. Its specific gravity and average particle diameter were 2.2 and 1 mm, respectively. The surface resistance of the GAC was measured at 2.3 Ω/cm^2 which may be conductive to facilitate electron transfer between microbial species. These physicochemical properties of the GAC in the cathode were expected to enhance biofilm growth and offer a conductive surface to enhance electrochemical performance of the E-AFMBR system. The inner wall of the reactor column was surrounded by titanium mesh as anode. The surface areas of cathode and anode were calculated based on the external surface area of the titanium mesh. Specifically, the cathode's surface area was 0.0456 m^2, and the anode's surface area was 0.0825 m^2. Distance between each electrode was 2 cm. The surface resistance of the titanium-based electrode measured by four-point meter (RC3175, EDTM, USA) was 0.5 Ω on average.

A Source/Measure unit (B2910BL, Keysight, USA) was connected to act as a power supply for applying external voltage onto the electrodes and monitoring current changes. In this study, the Source/Measure unit was used to continuously record current and resistance values in real time while a constant external voltage was applied. The current density was then calculated by dividing the measured current by the effective surface area of the activated cathode. The external voltage was selected in the range of −0.5 to +2.0 V, as this range is known to facilitate redox reactions in electrochemical MBR study [31]. A peristaltic pump (BT100-3J, Longer pump, China) was connected to the flat-tubular ceramic membrane and operated to produce permeate. A digital pressure gauge (KP-20, Sungji Tech, Korea) was connected between the membrane module and the peristaltic pump to monitor the TMP change with time. An additional peristaltic pump was used to provide feed solutions of synthetic greywater into the reactor. A level sensor was installed at the water level of the reactor to control feed and permeate pump automatically. Biogas produced by the AFMBRs was collected in a Tedlar bag (AS ONE, Japan) installed on reactor cover. A C-AFMBR was designed with the same reactor configuration as the E-AFMBR, including GAC particles packed in a titanium mesh serving as the cathode, a titanium electrode serving as the anode, PET beads, and a ceramic membrane. The only difference between the two systems was the application of external voltage. Under identical operating conditions, the C-AFMBR was operated under open circuit potential (OCP) without the application of external voltage, whereas the E-AFMBR was operated with an applied external voltage. This configuration was intended to quantitatively evaluate the effect of external voltage application on methane production efficiency and membrane fouling control.

2.2. Operating conditions

Before the start-up of reactor operation, both reactors were purged with nitrogen gas for 20 min to create an anaerobic environment. After nitrogen purging, each reactor was inoculated by adding 200 mL of seed sludge collected from the anaerobic digester operated at a local municipal wastewater treatment plant. The mixed liquor volatile suspended solid (MLVSS) concentration of the seed sludge was about 9400 mg/L.

Synthetic greywater was prepared as feed wastewater composed of sodium acetate anhydrous (CH_3COONa, Duksan, Korea), ammonium chloride (NH_4Cl, Duksan, Korea), dipotassium phosphate (K_2HPO_4, Samchun, Korea), sodium chloride (NaCl, Junsei, Japan), calcium chloride ($CaCl_2$, Daejung, Korea), and sodium dodecyl sulfate (SDS) ($C_{12}H_{25}NaO_4S$, Sigma-Aldrich, USA). In this study, SDS was chosen as a representative organic substance of the anionic surfactants which are commonly found in greywater. Soluble chemical oxygen demand (SCOD) concentration of feed wastewater applied in this study was about 320 mg/L. The concentration of SDS was about 10 mg/L. To maintain alkalinity, sodium bicarbonate ($NaHCO_3$, Daejung, Korea) was added into the feed wastewater periodically.

Reactors (E-AFMBR and C-AFMBR) were operated continuously over five distinct operational phases for 180 days (Table 1). During the operational period of Phase I (70 days), both the E-AFMBR and the C-AFMBR were operated at 16 h of HRT without SDS in feed wastewater. External voltage of −0.75 V was applied into the E-AFMBR. On day 71 of reactor operation, the SDS was added to the feed wastewater, and both reactors were then operated under the same HRT for 15 days (Phase II). After that, the HRT in both reactors were changed to 10 h and then operated in Phase III where the organic loading rate (OLR) increased from 0.492 to 0.803 gCOD/L·d. In Phase IV, the HRT was further reduced to 6 h, which corresponds to the OLR of 1.334 gCOD/L·d. The slight difference in OLR between Phase IV and V was due to small variations in the SCOD concentration as synthetic greywater was prepared. The average SCOD concentration throughout the operation was 323.09 ± 2.01 mg/L, resulting in a variation of less than 0.62 %, which is considered negligible to evaluate reactor performance. During the

Table 1
Operating parameters of both AFMBR systems.

Phase	I	II	III	IV	V
Period (d)	0–70	71–85	86–110	111–145	146–180
External voltage (V)[a]	−0.75	−0.75	−0.75	−0.75	−1.00
HRT (h)	16	16	10	6	6
Flow rate (L/d)	6.15	6.15	9.84	16.40	16.40
Permeate flux (L/m^2·h)	4.93	4.93	7.88	13.14	13.14
OLR (gCOD/L·d)	0.479	0.492	0.803	1.334	1.350
SDS concentration (mg/L)	–	10	10	10	10

[a] The external voltage was applied only to the E-AFMBR.

operational period of Phase V, the external voltage applied only to the E-AFMBR was increased to −1.00 V, and both reactors were operated under the same operational conditions as in Phase IV. The selection of external voltages (−0.75 and −1.00 V) was based on previous literature and theoretical considerations, as moderate electric fields (typically 0.4–1.0 V/cm) have been reported to reduce SMPs and extracellular polymeric substances (EPSs) concentrations, zeta potential, and sludge viscosity, thereby extending membrane lifespan while avoiding adverse effects on microbial activity [32–34].

2.3. Analytical methods

The SCOD concentrations of feed wastewater and membrane permeate were measured according to the Standard Methods [35]. All samples were prepared by filtering them through a 0.45 μm GD/X syringe filter (Cat. No. 6873-2504, Whatman™, UK). The MLVSS concentration in each reactor was also measured according to the Standard Methods [35]. For this, bulk samples were filtered through a 1.2 μm GF/C glass microfiber filter (Cat. No. 1822-047, Whatman™, UK). The SDS concentrations of feed wastewater and membrane permeate were determined by using the methylene blue active substance (MBAS) method [36] at a wavelength of λ_{max} = 652 nm with a UV–Visible spectrophotometer (Genesys 150, Thermo Scientific, USA). The pH of bulk solution in the reactor was measured by using a pH meter (Orion Star A214, Thermo Fisher Scientific, USA). The methane composition in the biogas produced from each AFMBR system was analyzed using a gas chromatograph-thermal conductivity detector (GC-TCD) (8890 GC system, Agilent Technologies, USA) equipped with a HayeSep D-packed column (G3591-80158, Agilent Technologies, USA). Volatile fatty acids (VFAs) of feed wastewater and membrane permeate were also measured by using a gas chromatograph-flame ionization detector (GC-FID) (8890 GC system, Agilent Technologies, USA) equipped with an HP-INNOWAX column (19091N-033, Agilent Technologies, USA). This study focused on the behavior of acetate ions among VFAs since sodium acetate anhydrous was used as the primary organic compound.

Both SMPs and EPSs have been measured to characterize organic substances that are derived from either microbial growth process or subsequent cell decay and lysis in AFMBR [11,37]. Samples were extracted as described in our previous study [11]. Proteins (PN) and polysaccharides (PS) were quantified by using the Phenol-Sulfuric acid method [38] and the modified Lowry-Folin method [39], respectively. The EPSs collected from each AFMBR were extracted to obtain soluble EPS (S-EPS), loosely-bound EPS (LB-EPS), and tightly-bound EPS (TB-EPS) fractions by centrifugation and sonication [40]. Samples were characterized by using three-dimensional excitation-emission matrix (EEM) spectrofluorometer (FP-8500ST, Jasco International, Japan). The EEM spectra were obtained by scanning the emission wavelengths from 200 to 600 nm while excitation wavelengths were varied from 200 to 400 nm at 2 nm increments. The acquired EEM data were analyzed and visualized with the Origin 2021 software v9.8.0.200 (OriginLab Corporation, USA). The particle size of foulants present in the bulk suspension was measured by using a laser particle size analyzer (Mastersizer 2000, Malvern Panalytical, UK). To identify and validate the impact of operational conditions on the AFMBR performance, a one-way analysis of variance (ANOVA) followed by Tukey's post-hoc test was conducted to determine statistically significant differences among operational phases. A significance level of $p < 0.05$ was used. To highlight gradual trends and progressive changes, statistical comparisons were limited to consecutive operational phases.

2.4. Microbial community analysis

Biomass samples were collected from the bulk suspension, anode biofilm, and cathode biofilm of each experimental reactor at the end of Phases III, IV, and V (days 110, 145, and 180). A 200 mL aliquot of the reactor bulk suspension was centrifuged at 10,000 *g* for 20 min, and the resulting pellet was resuspended in 5–10 mL of DNA/RNA Shield solution (Zymo Research, USA). Anode biomass was scraped from the surface of the titanium mesh anode and suspended in 5–10 mL of DNA/RNA Shield solution. Cathode biomass was collected by taking GAC particles from the cathode module and suspending them in 5–10 mL of DNA/RNA Shield solution. All collected samples were stored at −80 °C until subsequent analysis.

Total RNA extraction and cDNA synthesis from the biomass samples were carried out in one step using the SuperPrep II Cell Lysis & RT Kit for qPCR (TOYOBO, Japan), following the manufacturer's instructions. Before extraction, the stored cathode biomass samples were 4-fold concentrated after biofilm detachment by vortexing for 3 min. The 16S rRNA libraries for high-throughput sequencing (HTS) were prepared from the obtained cDNA samples by polymerase chain reaction (PCR) with universal prokaryotic primers 515F and 806R [41], each tagged with an Illumina adapter sequence at the 5' end, as previously described [42]. The resulting amplicon libraries were pooled into an equimolar mixture following the Illumina Metagenomic Sequencing Library Preparation instructions (Illumina, USA) and sent to Macrogen (Korea) for sequencing on the Illumina MiSeq platform. After discarding low-quality reads, the qualified reads were clustered into error-corrected amplicon sequence variants (ASVs), and their taxonomic affiliations were determined against the Ribosomal Database Project (RDP) database, as previously described [43]. The sequence data from this study were deposited in the NCBI Sequence Read Archive under BioProject accession number PRJNA1171123.

From the HTS data, one quantitative matrix was constructed for archaea and one for bacteria by considering the relative abundance of individual ASVs in each archaeal or bacterial library. Clustering analyses were performed on these matrices using the unweighted pair group method with arithmetic mean (UPGMA) algorithm, based on the Bray-Curtis dissimilarity, in PAST version 4.13 (https://www.nhm.uio.no/english/research/resources/past/).

2.5. Energy calculations

Each AFMBR requires energy to operate the peristaltic pump for the influent and permeate, as well as energy for media fluidization. However, since the peristaltic pump required for the influent water injection operates intermittently for a short period of time, the energy required here was excluded from this energy calculation using Eq. (1) [8]:

$$P = Q\gamma E \tag{1}$$

where P is the power requirement (W), Q is the flow rate (m^3/s), γ is the specific weight of clear water (9800 N/m^3), and E is the hydraulic pressure head loss (mH_2O). The power requirement was calculated based on the permeate volume treated per hour (m^3/h), and the energy consumption was estimated considering an electrical-to-pump energy conversion efficiency of 65 %.

In the case of the E-AFMBR, additional energy is required for external voltage, so this was calculated by applying Eq. (2) [44]:

$$W = \frac{UIt}{3600} \tag{2}$$

where W is the energy consumption of the power supply (Wh), U is the external voltage applied from the power supply (V), I is the mean current (A), and t is the operational time (h).

3. Results and discussion

3.1. TMP change with time

Fig. 2 compares the TMP measured by the E-AFMBR to those measured by the C-AFMBR during the whole operation period (180 d). In Phase I where HRT was 16 h corresponding to 4.93 $L/m^2 \cdot h$ (LMH) as

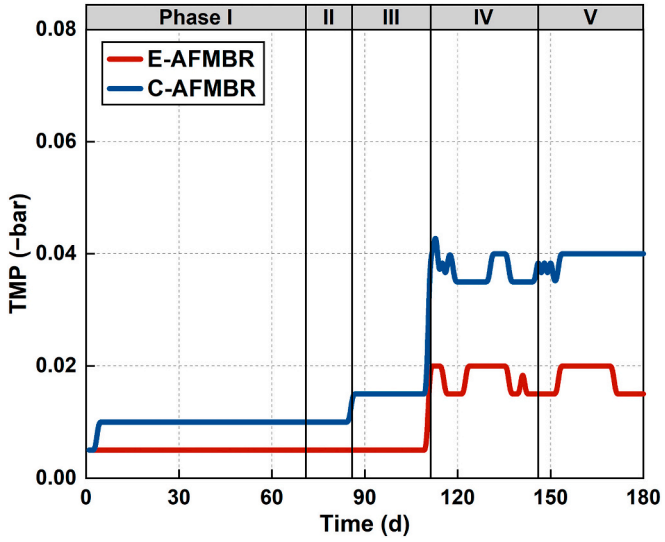

Fig. 2. The trend of TMP variation in each AFMBR over 180 days.

permeate flux, averaged TMP monitored in the E-AFMBR was 50 % lower than that in the C-AFMBR (−0.005 vs. −0.010 bar). Media fluidization with spherical PET beads worked very well in both reactors to maintain the TMP less than −0.1 bar. Moreover, applying external voltage of −0.75 V into the E-AFMBR provided synergistic impacts for enhancing antifouling efficiency. The bulk MLVSS concentration in the E-AFMBR was maintained below 50 mg/L during Phase I (Fig. S1). However, bulk MLVSS concentration in the C-AFMBR was about four times higher (200 mg/L), than that in the E-AFMBR. A possible explanation is that a significant portion of the biomass produced can be attached on the anode in the E-AFMBR. As SDS was injected into the feed wastewater for Phase II operation, no change in TMP was observed in both reactors. As the set-point flux increased to 7.88 LMH in Phase III, the TMP observed in the C-AFMBR increased to −0.015 bar, whereas it was only −0.005 bar in E-AFMBR. As the set-point flux increased to 13.14 LMH in Phase IV and V, the TMP in the E-AFMBR slightly increased to −0.020 while it rose rapidly to −0.040 bar in the C-AFMBR. During the whole operational period, bulk MLVSS concentration in the E-AFMBR reactor maintained always lower than that in the C-AFMBR (125.7 vs. 236.5 mg/L), thus employing lower fouling rate. These findings are consistent with previous studies on electrochemical anaerobic membrane bioreactors reporting that electrostatic repulsion can mitigate membrane fouling. However, in many of those studies, the fouling mitigation effect was limited during long-term reactor operation. As a result, additional cleaning methods that are not cost-effective, such as chemical cleaning, backwashing, or hydraulic cleaning were often necessary [19,44]. In contrast, the E-AFMBR system in this study demonstrated excellent long-term fouling control by maintaining low TMP without requiring such supplementary cleaning procedures. This performance is attributed to the combined effects of electrochemical reactions and mechanical cleaning actions achieved by external voltage applied and fluidized PET beads on membrane, respectively.

To understand the mechanisms behind fouling mitigation, a short-term filtration test was conducted using both reactors (see Fig. S2). In this experiment, membrane filtration was carried out without PET bead fluidization for the first 100 min, after which media fluidization along the membrane surface was initiated for 20 min. An external voltage of −1.00 V was applied to the E-AFMBR, while no voltage was applied to the C-AFMBR. During the initial 100 min of membrane filtration, the TMP increased by 0.10 bar with the E-AFMBR and 0.12 bar in the C-AFMBR. The average particle size in the bulk solution of the E-AFMBR was 21.5 μm, and this was approximately 2.3 times larger than that observed in the C-AFMBR (see Fig. S3). Small colloidal particles in the E-AFMBR underwent agglomeration due to electrocoagulation effects, likely induced by surface charge neutralization [45,46]. To support this observation, zeta potential was also measured at neutral pH. The particles in the E-AFMBR bulk solution were less negatively charged than those in the C-AFMBR (−13.50 mV vs. −17.50 mV, see Fig. S4). It is well known that a cake layer formed by larger particles has lower fouling resistance than one formed by smaller particles [46]. Consistent with this, the fouling rate in the E-AFMBR was 11 % lower than in the C-AFMBR (Fig. S2).

When mechanical cleaning was applied by PET bead fluidization in both systems, the TMP rapidly returned to its initial value within 20 min. These results suggest that the primary contributor to fouling reduction in the E-AFMBR was the mechanical cleaning action driven by fluidized PET beads, rather than electrostatic interactions alone. Under the operating conditions of Phase IV, where −0.75 V was applied to the E-AFMBR, the average particle size of bulk suspension was measured as 20.08 μm, and its zeta potential was −13.75 mV. These values were not significantly different from those measured under the −1.00 V condition in Phase V. Our observation was consistent with the fact that the TMP observed in the E-AFMBR during both phases were relatively stable (see Fig. 2). However, when compared to the C-AFMBR operated under the same conditions without any external voltage, the E-AFMBR showed noticeable differences in both particle size and zeta potential of reactor bulks.

Previous studies on membrane bioreactors combined with electrocoagulation (Electro-MBRs) have focused on the electrochemical mechanisms involved in fouling mitigation and changes in the physicochemical properties of suspended particles [47]. It has been reported that the application of an electric field reduced the surface charge (zeta potential) of suspended particles, thereby promoting particle aggregation and contributing to fouling reduction. In Electro-MBRs, the zeta potential of suspended particles was reported to range from approximately −6.5 mV to −17.5 mV, whereas in control-MBRs operated without an electric field, it ranged from −17.5 mV to −21.5 mV. This indicates that the electric field in the Electro-MBR may neutralize the surface charges of the suspended particles, thus enhancing inter-particle aggregation and formation of a loosely bound cake structure. Additionally, the same study was also noted that the electrocoagulation process could enhance the adsorption of soluble foulants, particularly S-EPS, thus contributing to mitigate membrane fouling [47]. The EPS concentration in the E-AFMBR remained consistently lower than that in the C-AFMBR throughout the entire operational period (Table S1). Therefore, the electrokinetic effects within the E-AFMBR may play a significant role in reducing membrane fouling by altering key physicochemical properties of the suspended particles, such as surface charge and particle size. These findings suggest that the presence of an electric field can serve as a crucial factor to control fouling resistance in membrane bioreactor systems.

In Phase IV, the SMP protein (SMP_{PN}) concentration in the reactor was measured to be 41.3 mg/L in the E-AFMBR and 45.3 mg/L in the C-AFMBR (see Table S1 of Supplementary Data). The EPS protein (EPS_{PN}) concentration of the C-AFMBR bulk solution was 1.8 times higher than that in the E-AFMBR. In both SMPs and EPSs, carbohydrates were not observed in either reactor. As a result of EEM analysis, an excitation-emission peak related to LB-EPS was observed at 200–250 nm in the case of the E-AFMBR and 200–240 nm in the case of the C-AFMBR (Fig. 3). The difference in peak intensity is thought to be due to the difference in the degree of decomposition of aromatic amino acids, such as tyrosine, present in greywater [48]. Aromatic amino acids can be synthesized via biosynthesis or the shikimate pathway [49]. The lower intensity of the EEM peak related to the aromatic amino acids in the E-AFMBR than that in the C-AFMBR may be caused by the fact that the organic compound can be degraded effectively by electrochemical oxidation. Aromatic amino acids containing a benzene ring can be effectively oxidized by electrochemically generated hydroxyl radicals [50,51]. The mechanism of organic acid occurring in the E-AFMBR is

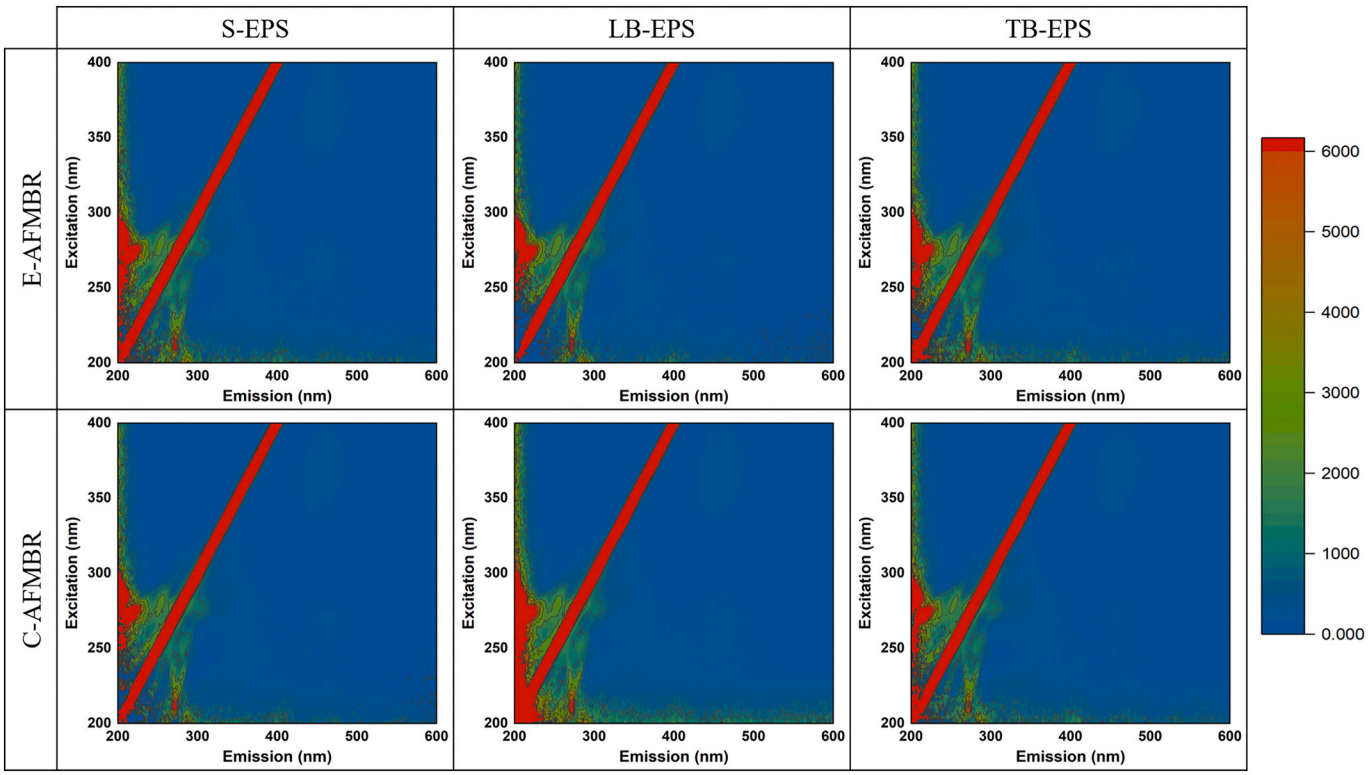

Fig. 3. 3D-EEM spectra of bulk suspensions collected from each AFMBR in Phase IV.

discussed in detail in Section 3.3.

3.2. Organic removal

The comparative results of SCOD removal efficiency over the entire operational period are shown in Fig. 4. During the initial phase of operation, SCOD removal was not significantly influenced by membrane filtration alone, given the negligible contribution of porous microfiltration (MF) membranes to rejecting organic compounds [52]. Instead, these initial organic removal efficiencies in both the E-AFMBR and the C-AFMBR were thought to be primarily attributed to biosorption of organic compounds onto bio-flocs formed in the reactors and/or the adsorption provided by GAC particles enclosed in titanium mesh [10].

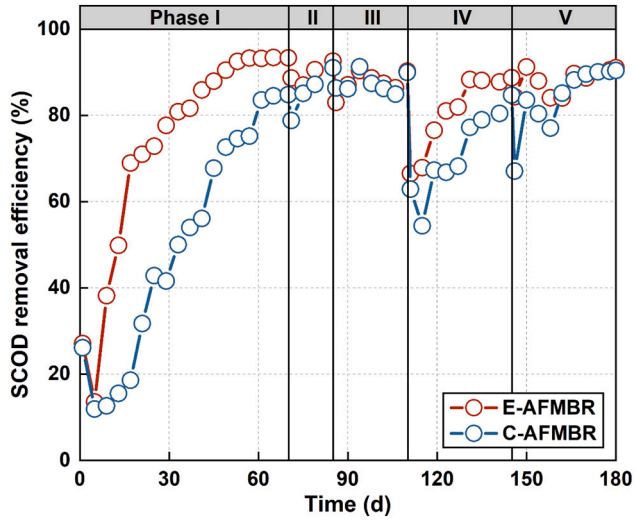

Fig. 4. SCOD removal efficiency of each AFMBR over 180 days.

However, since both reactors contained the same amount of GAC particles, the adsorptive behavior of organic compounds onto GAC is unlikely to account for the different performances observed between the E-AFMBR and the C-AFMBR. As the operation time was extended, however, SCOD removal efficiencies exceeded 80 % by day 70. Nevertheless, the extent of SCOD removal was improved more by the E-AFMBR than by the C-AFMBR. These results were consistent with our observations on transient behavior of SCOD removal efficiency in the E-AFMBR, particularly during Phase I as initial stage and Phase IV when HRT was reduced.

Although both systems eventually showed a similar steady-state performance, the E-AFMBR exhibited a faster initial response on higher SCOD removal, likely due to electrochemical oxidation facilitated by the applied voltage. This enhanced performance was attributed to the activity of electroactive bacteria present in the E-AFMBR, which enabled more efficient electron transfer pathways along with a minor contribution from electrochemical oxidation under the applied voltage (−0.75 V) [53,54]. Once microbial activity was stabilized, however, the differences associated with SCOD removal efficiency between the two reactors were gradually diminished, indicating that anaerobic microbial metabolism became the dominant organic removal mechanism as operation time progressed.

Following SDS addition in Phase II, SCOD removal efficiency dropped by 5–6 % in both systems. This is consistent with previous findings that SDS can temporarily inhibit anaerobic microbial activity by disrupting cell membranes [10]. However, the E-AFMBR showed faster recovery (92.6 %) compared to the C-AFMBR (91.0 %) by the end of Phase II, suggesting improved resilience likely supported by both biofilm stability and the presence of electrochemically active zones. During Phase IV, when the HRT was reduced to 6 h (1.334 gCOD/L·d of OLR), both systems experienced a sharp decline to 60 % in SCOD removal. However, the E-AFMBR recovered more quickly, reaching 90 % removal within a shorter timeframe. This suggests that the applied voltage may have supported microbial adaptation under high loading stress through enhanced redox activity and retention of syntrophic associations, as

reported in similar electrochemical MBR studies [55]. Furthermore, the consistent high SDS removal efficiency (>90 %) observed in both reactors throughout Phases II to V indicates that SDS is readily biodegradable in the AFMBR systems, regardless of electrochemical conditions. Statistically significant differences ($p < 0.05$) in SCOD removal efficiency were observed between Phases I and II, Phases III and IV, and Phases IV and V. These differences can be attributed to the addition of SDS, the reduction of HRT to 6 h, and the increase in applied external voltage to −1.00 V, respectively. In contrast, the difference between Phases II and III was not statistically significant ($p = 0.2121$), suggesting that the change in HRT from 12 to 10 h had a limited impact on microbial metabolism and thus showing a similar level of SCOD removal efficiency. A similar lack of statistical significance was also observed in the C-AFMBR between Phases II and III ($p = 0.5170$), indicating consistent performance under these conditions. Overall, although both systems ultimately achieved similar steady-state SCOD removal, the E-AFMBR demonstrated faster responses during perturbation and early operation, highlighting the operational advantage of electrochemical integration during non-steady-state conditions.

3.3. Methane production

Fig. 5 compares the methane production profiles of the E-AFMBR and the C-AFMBR over the entire operational period. In both systems, methane production rates increased with decreasing HRT, primarily due to elevated OLRs. Notably, the E-AFMBR consistently exhibited a higher rate in methane production than the C-AFMBR. In Phase V, increasing the external voltage from −0.75 V to −1.00 V resulted in methane production rate at 49.9 % higher in the E-AFMBR than the C-AFMBR. This enhancement can be attributed to multiple mechanisms. First, our microbial community analysis (see Section 3.5) revealed a higher abundance of *Geobacter* and *Methanobacterium*, which are electroactive microorganisms known to facilitate direct interspecies electron transfer (DIET). The presence of an electric field promotes DIET by enhancing redox conditions which favor electron exchange between syntrophic partners [53,54]. Second, the external voltage applied into the E-AFMBR can facilitate the oxidation of complex organics into the intermediates which are readily biodegradable such as acetate, thereby increasing the substrate availability for methanogens [56]. Faster depletion of acetic acid as observed in the E-AFMBR during Phases I and III can support that anodic respiration should be enhanced by electroactive bacteria (Fig. S5). Furthermore, gas composition in the biogas produced by the E-AFMBR had lower CO_2 content than that by the C-AFMBR from Phases II to V (Fig. S6). This observation was related to our results showing dominance of *Methanobacterium*, which is capable of both hydrogenotrophic and electrotrophic methanogenesis, in the cathodic biofilm (see Section 3.5). This genus is capable of performing both hydrogenotrophic and electrotrophic methanogenesis because they are well known to reduce CO_2 to CH_4 through either hydrogen or cathodic electrons. Therefore, the lower CO_2 content in the biogas produced by the E-AFMBR than the C-AFMBR is likely attributable to enhanced CO_2 reduction to CH_4, supporting our results that the external voltage applied in the E-AFMBR boosts methane production.

Although methane production was dropped temporarily with both reactors during Phases III and IV due to microbial sampling events, methane production recovery resumed within five days as anaerobic conditions were reestablished. Meanwhile, the methane production rate in the E-AFMBR showed statistically significant differences ($p < 0.05$) across all operational phases, indicating that each operational change to methane production should be meaningful. In contrast, the C-AFMBR showed a p-value of 0.2671 between Phases IV and V during which no operational changes were applied, suggesting that the difference in reactor performance during this period was not statistically significant. To support these findings, a comparative analysis with recent studies further highlighted the effectiveness of the E-AFMBR system in terms of enhancing methane recovery. For instance, a previous study on electrochemical anaerobic membrane bioreactor demonstrated a methane yield of 0.217 L/gSCOD$_{removed}$ at an OLR of 0.597 gCOD/L·d at applied voltage of 0.8 V [55]. By contrast, the E-AFMBR in this study achieved a higher methane yield of 0.278 L/gSCOD$_{removed}$ at a slightly lower voltage of −0.75 V, despite the reactor was operated at a higher OLR of 1.350 gCOD/L·d. Overall, the superior methane production in the E-AFMBR to the C-AFMBR can be attributed to the synergistic effects of accelerated DIET, biodegradability improved by electrochemical oxidation, and effective CO_2 utilization. These results underscored the multiple advantages of electrochemical integration to enhance methanogenic performance in the E-AFMBR treating greywater.

3.4. Change of current density

Fig. 6 shows the change in current density observed at the cathode during the E-AFMBR operational period. As soon as a seed sludge was injected into the E-AFMBR, the current density rapidly increased to 0.726 A/m^2 (based on cathode surface area) by the 13th day of operation. During this period, the bulk MLVSS concentration was observed to be 100 mg/L, and this was about 55 % of the bulk MLVSS concentration of the C-AFMBR during the same operational period (Fig. S1). These

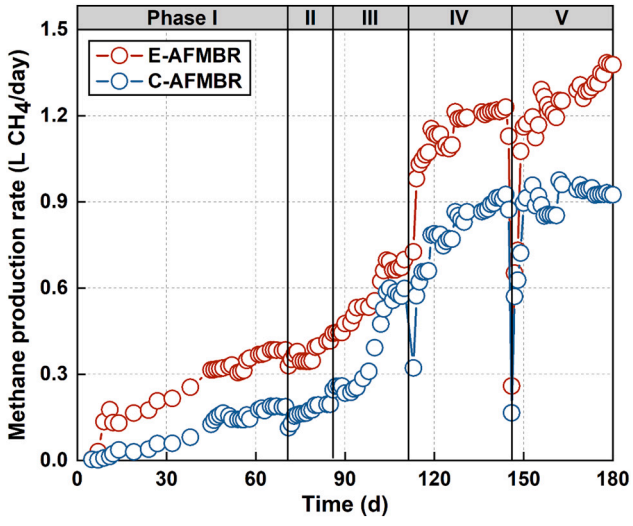

Fig. 5. Methane production rates in E-AFMBR and C-AFMBR over 180 days.

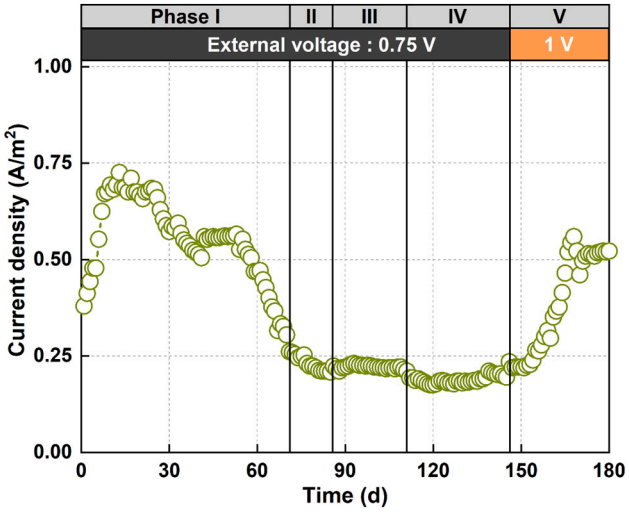

Fig. 6. Variation in the current density of E-AFMBR over the entire operation period.

results suggest that microorganisms carrying negative charges may grow at the anode in the E-AFMBR system [57]. In particular, electroactive bacteria grown on the anode surface are thought to decompose the substrate, thereby enhancing extracellular electron transfer and thus increasing the current density [21,58]. The seed sludge inoculated into the E-AFMBR was composed of 2.09 % *Geobacter* and 0.75 % *Desulfovibrio*, both of which are well-known as electroactive bacteria (Fig. S7).

During the initial 15-day operation period, total SMP and EPS concentrations in the E-AFMBR were 6.1 and 2.2 mg/L, respectively, indicating that current density between the electrodes was not significantly affected by microbial activity by-products (Table S1). After the initial operational stage, however, the concentrations of microbial by-products such as EPSs and SMPs gradually increased, which also increased the resistance between the electrodes and decreased the current density as shown in Fig. 6. The current density measured in the E-AFMBR decreased to 0.305 A/m^2 at the end of Phase I, but total SMP and EPS concentrations increased to 27.1 and 21.6 mg/L, respectively. A decrease in current density can lower coulombic efficiency because the electrons produced during the organic oxidation process cannot be effectively transferred to the anode. During Phases II and III, the current densities of the E-AFMBR bulk solution were observed to be 0.231 and 0.222 A/m^2 on average, respectively. When the HRT was reduced to 6 h, the SMP and EPS concentrations increased to 41.3 and 51.2 mg/L, which were 1.76 and 3.16 times higher than them when HRT was 10 h. Increasing the concentration of SMPs and EPSs increased the interelectrode resistance from 74.2 to 87.3 Ω and decreased the current density to 0.189 A/m^2 on average. The current density at the cathode observed in Phase V increased to 0.522 A/m^2 when the external voltage increased to −1.00 V, but the SMP and EPS concentrations decreased to 25.7 and 32.8 %, respectively, compared to the concentrations observed in the previous operation phase. Although current densities previously reported in electrochemical MBR systems range from 2.5 to 15 A/m^2 [34,59,60], it is important to note that current density is influenced by several interrelated factors such as electrode material and configuration, interelectrode distance, reactor architecture, and the physicochemical characteristics of the bulk solution (e.g., conductivity, viscosity, and organic loading). Despite operating at a relatively lower current density compared to those reported in the literature, the E-AFMBR system in this study maintained stable operation and consistent organic matter removal efficiency throughout the experimental period.

3.5. Microbial community analysis

A total of 1,537,398 bacterial reads and 380,605 archaeal HTS reads were obtained, identifying 6708 bacterial ASVs and 218 archaeal ASVs. Microbial community structures varied greatly between the reactors and sampling locations (i.e., bulk suspension, anode biofilm, and cathode biofilm) (Fig. 7), highlighting the critical influence of external voltage application on shaping their microbial communities. These variations are clearly illustrated in the cluster dendrograms of archaeal and bacterial communities (Fig. S8).

Nearly all archaeal HTS reads (99.6 %) were assigned to two methanogen genera: acetoclastic *Methanothrix* and hydrogenotrophic *Methanobacterium*. These genera dominated the archaeal communities in both the C-AFMBR and the E-AFMBR, collectively representing 78.3–95.2 % relative abundance (based on 16S rRNA read counts). Notably, the cathodic archaeal community of the E-AFMBR consistently exhibited a distinct structure, with *Methanobacterium* overwhelmingly dominant (>70 % relative abundance), whereas *Methanothrix* was the most abundant archaeal genus in all other reactor biomass samples (>58 % relative abundance). This difference suggests that the cathodic environment promoted the enrichment of *Methanobacterium*. Given that this genus is capable of reducing CO_2 to methane electrotrophically as well as hydrogenotrophically [61], its dominant growth was potentially supported by electrons and hydrogen derived from the cathode [62]. These results suggest that the applied voltage likely enhanced both direct and indirect electron transfer for CO_2 reduction to methane [63], contributing to the higher methane production in the E-AFMBR compared to the C-AFMBR. Meanwhile, the dominance of *Methanothrix* in the bulk suspensions and anode biofilms of both reactors is consistent with acetate being the primary carbon source in the feed wastewater. Of note is that *Methanothrix* is also capable of electrotrophic methanogenesis and often involved in electric syntrophy with exoelectrogenic bacteria in anaerobic digestion environments [64]. Therefore,

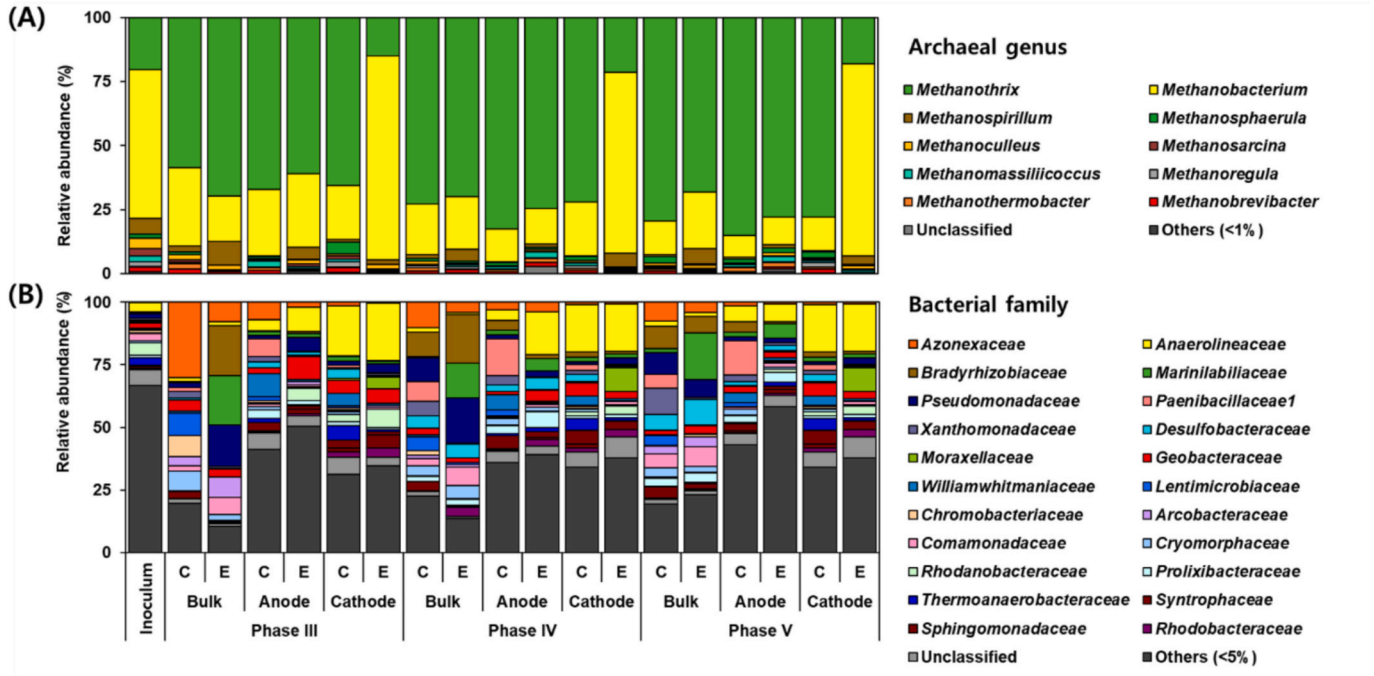

Fig. 7. Taxonomic distribution of archaeal (A) and bacterial (B) sequences in each 16S rRNA library. Archaeal ASVs with less than 1 % relative abundance at the genus level and bacterial ASVs with less than 5 % at the family level were grouped as 'Others'. 'C' represents C-AFMBR, and 'E' represents E-AFMBR.

Methanothrix in the cathode biofilm of the E-AFMBR may have partially supported the conversion of CO_2 into methane through the electrotrophic pathway, despite its substantially lower relative abundance in the cathode biofilm of the E-AFMBR compared to the C-AFMBR.

Compared to archaea, bacteria exhibited significantly more dynamic variations in community structure across biomass samples from different reactors and sampling locations (Figs. 7B and S8). This difference can be attributed to the limited taxonomic diversity and narrow substrate spectrum of methanogens [65]. In both reactors, *Azonexaceae* (4.1–30.1 %) and *Pseudomonadaceae* (1.7–18.3 %) were prominent bacterial families in the bulk suspension communities. Members of these families are capable of degrading complex organic compounds into simple organic molecules under anaerobic conditions [66,67]. Meanwhile, in the electrode biofilms, the well-known exoelectrogenic bacterial family *Geobacteraceae* (1.3–9.2 %) was enriched. Bacteria from this family likely played an essential role in transferring substrate-derived electrons to the anode and electrotrophic microorganisms. Representative exoelectrogenic genera, such as *Geobacter*, *Desulfovibrio*, and *Shewanella*, were prevalent across all tested biomass samples, showing generally higher relative abundance in the electrode biofilms (Fig. S7). Specifically, the primary exoelectrogenic genus *Geobacter* exhibited significantly higher relative abundance in the anode biofilm of the E-AFMBR (2.4–9.2 %) compared to the C-AFMBR (1.3–2.6 %), reflecting the promotion of anodic respiration by the applied voltage. *Geobacter* was also abundant in the cathodic biofilms of both reactors, with higher relative abundance in the cathode biofilm (4.4–5.1 %) than in the anode biofilm of the C-AFMBR. This result suggests the development of electric syntrophy between exoelectrogenic bacteria, primarily *Geobacter*, and their syntrophic partners, including *Methanobacterium* and *Methanothrix*, through DIET mediated by electrically conductive GAC in the cathode biofilms [61,68]. The combined enhancement of anodic respiration and electrosyntrophic methanogenesis appears to have resulted in improved organic removal and methane production in the E-AFMBR compared to the C-AFMBR. These results demonstrate that the external voltage application had a significant impact on the evolution and behavior of suspended, anodic, and cathodic microbial communities, directly influencing the reactor performance.

Additionally, sulfate-reducing bacteria, such as the families *Desulfobacteraceae* (0.1–10.2 %), *Desulfobulbaceae* (0.0–2.0 %), *Desulfovibrionaceae* (0.2–1.8 %), were commonly observed in both reactors across the bulk suspension and electrode biofilms (Fig. 7B). These bacteria likely contributed to SDS degradation by scavenging sulfate released during its decomposition [69] with *Anaerolineaceae* populations potentially involved in breaking down SDS [31]. Notably, *Desulfovibrionaceae* was represented by the exoelectrogenic and hydrogenic genus *Desulfovibrio* [70]. With higher relative abundance in the electrode biofilms compared to the bulk suspension (Fig. S7), *Desulfovibrio* likely contributed to anodic respiration as well as electron transfer, both directly and via hydrogen, to methanogens.

3.6. Energy balance

The results of energy balance calculation during the Phase V operation are shown in Table 2. Both reactors require the same amount of energy for media fluidization because they use the same PET beads at the same packing ratio. When comparing only the amount of energy required to operate a permeation pump, the energy required was 0.041 and 0.109 Wh/m^3 in the E-AFMBR and the C-AFMBR, respectively. As shown in Table 2, most operating energy for both reactors were consumed for media fluidization. The total energy required for the operation of the E-AFMBR and the C-AFMBR was 33.81 and 33.88 Wh/m^3, respectively. The energy required to apply external voltage to the E-AFMBR was approximately 0.01 Wh/m^3. Considering energy transfer efficiency (65 %), the total amount of energy consumed by the E-AFMBR and the C-AFMBR was 52.03 and 52.13 Wh/m^3, respectively. The sensitivity analysis conducted across all operational phases revealed a consistent decrease in total energy consumption in both the E-AFMBR and the C-AFMBR systems as the HRT was reduced from 16 to 6 h. Specifically, in the E-AFMBR, total energy consumption decreased from 90.06 Wh/m^3 at 16 h (Phase I) to 33.77 Wh/m^3 at 6 h (Phase V), representing a 62.5 % reduction. This decline was primarily attributed to the reduced energy demand for PET bead fluidization per unit volume of treated water, as shorter HRTs increased the permeate flux. In contrast, the energy required for membrane permeation and external voltage application accounted for less than 1 % of the total energy consumption, with contributions of 0.121 and 0.029 %, respectively. These results indicate that HRT is the most influential operational parameter affecting overall energy demand in the long-term operation of the E-AFMBR system.

Table 2
Energy balance of E-AFMBR and C-AFMBR in Phase V.

	E-AFMBR	C-AFMBR
(a) Electrical energy consumption		
1. Energy consumption for PET beads fluidization		
1.1. Reactor head loss (mH_2O)	7.85×10^{-3}	
1.2. Reactor recirculation flow rate (m^3/s)	3.00×10^{-4}	
1.3. Fluidization energy consumption (W)	2.31×10^{-2}	
1.4. Consumed pumping energy (Wh/m^3)	33.77	
2. Energy consumption for permeation		
2.1. Average TMP (mH_2O)	1.50×10^{-2}	4.00×10^{-2}
2.2. Permeate flow rate (m^3/s)	1.90×10^{-7}	
2.3. Permeation energy consumption (W)	2.79×10^{-5}	7.44×10^{-5}
2.4. Consumed pumping energy (Wh/m^3)	0.041	0.109
3. Energy consumption for power supply		
3.1. External voltage (V)	1.0	–
3.2. Average current (A)	2.38×10^{-2}	–
3.3. Power supply energy consumption (Wh)	6.61×10^{-6}	–
3.4. Consumed electric energy (Wh/m^3)	9.67×10^{-3}	–
Total electrical energy consumption (Wh/m^3)[a]	52.03	52.13
(b) Electrical energy production		
1. Influent concentration (mgSCOD/L)	333	
2. Permeate flow rate (L/d)	16.40	
3. Biogas yield (L/d)	1.660	1.300
3. Biogas yield (mol/d)	0.074	0.058
3. Biogas yield (mol/m^3)	4.519	3.539
4. Methane gas composition (%)	82.99	71.16
5. Produced methane gas (mol/m^3)	3.750	2.518
6. Methane energy content (Wh/m^3)[b]	832.5	559.0
Electrical recovery from methane gas (Wh/m^3)[c]	275	184
Energy balance	528 %	354 %

[a] The energy transfer efficiency for converting electrical energy to pump energy is assumed to be 65 % [71].
[b] The theoretical energy obtainable from the produced gaseous methane is 0.222 kWh per mole, where 1 mol of CH_4 is equivalent to 64 gCOD [8].
[c] The energy conversion efficiency from methane to electricity is assumed to be 33 % [8].

The amount of electrical energy that can be converted from methane produced by each reactor operated at 6 h of HRT is shown in Table 2b. The amount of gaseous methane produced by the E-AFMBR and the C-AFMBR was 3.750 and 2.518 mol CH_4/m^3 wastewater, respectively, which correspond to methane yields of 0.278 and 0.188 L CH_4/gSCOD$_{removed}$. Considering all the methane produced could be converted into electrical energy, the electricity recovered from the methane produced by the E-AFMBR and the C-AFMBR was 275 and 184 Wh/m^3, respectively. When considering the percentage of energy production to consumption ratio, the E-AFMBR and the C-AFMBR showed 528 % and 354 % indicating that the E-AFMBR should have 1.49 times higher energy productivity than that of the C-AFMBR. In addition, our results revealed that the electrical energy recovered by the E-AFMBR increased from 205 to 245 Wh/m^3, representing an approximate 19.5 % increase as the HRT was reduced from 16 h (Phase I) to 6 h (Phase IV). Under the same conditions, the C-AFMBR system showed an increase from 100 to 174 Wh/m^3. Furthermore, when the applied external voltage in the E-

AFMBR was increased from −0.75 V to −1.00 V in Phase V, electrical energy recovery further increased to 275 Wh/m^3, indicating an additional 12.2 % improvement after applying higher voltage input.

This electrical energy recovery was significantly higher than that reported in a previous study using a conventional AFMBR without external voltage for synthetic greywater treatment, in which PET beads were applied as fluidized media. That study showed an energy balance of 209 % at an HRT of 8 h [10]. In contrast, we achieved an energy balance of 528 % using the E-AFMBR at a shorter HRT of 6 h, clearly demonstrating that the integration of electrochemical technology significantly enhanced energy performance. The net energy recovery, calculated by subtracting total electrical energy consumption from the electrical energy recovered from methane production (assuming a 33 % electricity conversion efficiency), was 222.97 Wh/m^3 for the E-AFMBR and 131.87 Wh/m^3 for the C-AFMBR.

4. Conclusions

In this study, an E-AFMBR was developed to address the limitations of conventional AFMBRs in greywater treatment, particularly with respect to membrane fouling, organic removal, and methane production. The application of external voltage improved membrane fouling control by over 50 %, mainly due to electrostatic repulsion, electrocoagulation, and electrochemical oxidation of microbial by-products. However, the reduction in membrane fouling in the E-AFMBR was attributed more to the mechanical scouring effect caused by the fluidization of PET beads than to electrostatic interactions, which enabled stable long-term reactor operation. Both the E-AFMBR and the C-AFMBR achieved similar organic removal efficiencies over 90 % after reaching steady-state conditions. However, the E-AFMBR demonstrated a faster rate of organic removal than the C-AFMBR, particularly during the initial stabilization period and recovery phases, likely due to electrochemical reactions induced by the applied external voltage. Methane production was 48.9 % higher in the E-AFMBR compared to the C-AFMBR, as supported by microbial community analysis identifying *Geobacter* and *Methanobacterium* as dominant electroactive bacteria involved in DIET. Furthermore, the E-AFMBR achieved a high energy recovery rate of 528 % and exhibited consistent performance under varying HRT conditions, indicating its strong potential as a decentralized greywater treatment technology. Future research should focus on scaling up the E-AFMBR and conducting demonstration studies using real greywater to assess its applicability in practical decentralized wastewater treatment systems.

CRediT authorship contribution statement

Minseok Kim: Writing – original draft, Methodology, Investigation, Formal analysis, Data curation. **Dayoung Ko:** Writing – original draft, Methodology, Investigation, Formal analysis, Data curation. **Minyeong Lee:** Methodology, Investigation, Formal analysis. **Changsoo Lee:** Writing – review & editing, Formal analysis, Conceptualization. **Jeonghwan Kim:** Writing – review & editing, Supervision, Funding acquisition, Formal analysis, Conceptualization.

Declaration of competing interest

The authors declare that they have no known competing financial interests or personal relationships that could have appeared to influence the work reported in this paper.

Acknowledgement

This work was supported by the National Research Foundation of Korea (NRF) grants funded by the Korean Government (MSIT) (RS-2022-NR070367, RS-2025-02213817).

Appendix A. Supplementary data

Supplementary data to this article can be found online at https://doi.org/10.1016/j.cej.2025.167254.

Data availability

No data was used for the research described in the article.

References

[1] G. Skouteris, D. Hermosilla, P. López, C. Negro, Á. Blanco, Anaerobic membrane bioreactors for wastewater treatment: a review, Chem. Eng. J. 198 (2012) 138–148.
[2] S. Vinardell, S. Astals, M. Peces, M. Cardete, I. Fernández, J. Mata-Alvarez, J. Dosta, Advances in anaerobic membrane bioreactor technology for municipal wastewater treatment: a 2020 updated review, Renew. Sustain. Energy Rev. 130 (2020) 109936.
[3] A. Arias, G. Feijoo, M.T. Moreira, Environmental profile of decentralized wastewater treatment strategies based on membrane technologies, in: Current Developments in Biotechnology and Bioengineering, Elsevier, 2020.
[4] L. Rodríguez-Hernández, M. González-Viar, L. De Florio, I. Tejero, Hybrid membrane bioreactor application for decentralized treatment and reuse, Desalin. Water Treat. 51 (10–12) (2013) 2467–2473.
[5] A. Van de Walle, M. Kim, M.K. Alam, X. Wang, D. Wu, S.R. Dash, K. Rabaey, J. Kim, Greywater reuse as a key enabler for improving urban wastewater management, Environ. Sci. Ecotechnol. 16 (2023) 100277.
[6] C. Shin, J. Bae, Current status of the pilot-scale anaerobic membrane bioreactor treatments of domestic wastewaters: a critical review, Bioresour. Technol. 247 (2018) 1038–1046.
[7] S. Vinardell, L. Sanchez, S. Astals, J. Mata-Alvarez, J. Dosta, M. Heran, G. Lesage, Impact of permeate flux and gas sparging rate on membrane performance and process economics of granular anaerobic membrane bioreactors, Sci. Total Environ. 825 (2022) 153907.
[8] J. Kim, K. Kim, H. Ye, E. Lee, C. Shin, P.L. McCarty, J. Bae, Anaerobic fluidized bed membrane bioreactor for wastewater treatment, Environ. Sci. Technol. 45 (2) (2011) 576–581.
[9] M. Aslam, P.L. McCarty, C. Shin, J. Bae, J. Kim, Low energy single-staged anaerobic fluidized bed ceramic membrane bioreactor (AFCMBR) for wastewater treatment, Bioresour. Technol. 240 (2017) 33–41.
[10] M. Kim, S.W. How, S.R. Dash, D. Wu, J. Kim, Membrane fouling, methane production and microbial community under fluidization of biocarrier with conductive surface in anaerobic fluidized bed membrane bioreactor for greywater treatment, J. Membr. Sci. 688 (2023) 122108.
[11] M. Kim, T.Y. Lam, G.-Y.A. Tan, P.-H. Lee, J. Kim, Use of polymeric scouring agent as fluidized media in anaerobic fluidized bed membrane bioreactor for wastewater treatment: system performance and microbial community, J. Membr. Sci. 606 (2020) 118121.
[12] W. Cai, Y. Du, J. Wang, Development of innovative hydrogel-GAC particles utilized in aerobic fluidized bed membrane bioreactor for enhancing high-saline organic wastewater treatment, J Water Process Eng 68 (2024) 106416.
[13] N. LaBarge, Y. Ye, K.-Y. Kim, Y.D. Yilmazel, P.E. Saikaly, P.-Y. Hong, B.E. Logan, Impact of acclimation methods on microbial communities and performance of anaerobic fluidized bed membrane bioreactors, Environ. Sci.: Water Res. Technol. 2 (6) (2016) 1041–1048.
[14] A. Charfi, E. Park, M. Aslam, J. Kim, Particle-sparged anaerobic membrane bioreactor with fluidized polyethylene terephthalate beads for domestic wastewater treatment: modelling approach and fouling control, Bioresour. Technol. 258 (2018) 263–269.
[15] Y.A. Tayeh, M.Y. Alazaiza, T.M. Alzghoul, M.J. Bashir, A comprehensive review of RO membrane fouling: mechanisms, categories, cleaning methods and pretreatment technologies, J. Hazard. Mater. Adv. 18 (2025) 100684.
[16] S. Theuri, K. Gurung, V. Puhakka, D. Anjan, M. Sillanpaa, Effect of temperature variations in anaerobic fluidized membrane bioreactor: membrane fouling and microbial community dynamics assessment, Int. J. Environ. Sci. Technol. 20 (9) (2023) 9451–9464.
[17] A. Lago, V. Rocha, O. Barros, B. Silva, T. Tavares, Bacterial biofilm attachment to sustainable carriers as a clean-up strategy for wastewater treatment: a review, J Water Process Eng 63 (2024) 105368.
[18] X.-B. Ying, J.-J. Huang, D.-S. Shen, H.-J. Feng, Y.-F. Jia, Q.-Q. Guo, Fouling behaviors are different at various negative potentials in electrochemical anaerobic membrane bioreactors with conductive ceramic membranes, Sci. Total Environ. 761 (2021) 143199.
[19] K. Zhao, F. Su, K. Gu, J. Qi, R. Liu, C. Hu, Antifouling potential and microbial characterization of an electrochemical anaerobic membrane bioreactor utilizing membrane cathode and iron anode, Bioresour. Technol. 334 (2021) 125230.
[20] Z. An, J. Zhu, M. Zhang, Y. Zhou, X. Su, H. Lin, F. Sun, Anaerobic membrane bioreactor for the treatment of high-strength waste/wastewater: a critical review and update, Chem. Eng. J. 470 (2023) 144322.
[21] M. Cao, Y. Zhang, Y. Zhang, Effect of applied voltage on membrane fouling in the amplifying anaerobic electrochemical membrane bioreactor for long-term operation, RSC Adv. 11 (50) (2021) 31364–31372.

[22] C.M. Werner, K.P. Katuri, A.R. Hari, W. Chen, Z. Lai, B.E. Logan, G.L. Amy, P. E. Saikaly, Graphene-coated hollow fiber membrane as the cathode in anaerobic electrochemical membrane bioreactors–effect of configuration and applied voltage on performance and membrane fouling, Environ. Sci. Technol. 50 (8) (2016) 4439–4447.
[23] Y. Yang, S. Qiao, R. Jin, J. Zhou, X. Quan, Novel anaerobic electrochemical membrane bioreactor with a CNTs hollow fiber membrane cathode to mitigate membrane fouling and enhance energy recovery, Environ. Sci. Technol. 53 (2) (2018) 1014–1021.
[24] F. Anjum, I.M. Khan, J. Kim, M. Aslam, G. Blandin, M. Heran, G. Lesage, Trends and progress in AnMBR for domestic wastewater treatment and their impacts on process efficiency and membrane fouling, Environ. Technol. Innov. 21 (2021) 101204.
[25] Y. Yang, S. Qiao, R. Jin, J. Zhou, X. Quan, Fouling control mechanisms in filtrating natural organic matters by electro-enhanced carbon nanotubes hollow fiber membranes, J. Membr. Sci. 553 (2018) 54–62.
[26] C. Hou, L. Du, D. Chen, X. Zhao, J. Zhou, S. Qiao, The preparation of electrically-enhanced and hydrophilic CNTs-PVDF composite hollow fiber membranes for fouling resistance, Sep. Purif. Technol. 351 (2024) 127968.
[27] D. Hu, L. Liu, W. Liu, L. Yu, J. Dong, F. Han, H. Wang, Z. Chen, H. Ge, B. Jiang, Improvement of sludge characteristics and mitigation of membrane fouling in the treatment of pesticide wastewater by electrochemical anaerobic membrane bioreactor, Water Res. 213 (2022) 118153.
[28] L. Wang, Y. Wu, Y. Fu, L. Deng, Y. Wang, Y. Ren, H. Zhang, Low electric field assisted surface conductive membrane in AnMBR: strengthening effect and fouling behavior, Chem. Eng. J. 431 (2022) 133185.
[29] K.-Y. Kim, W. Yang, Y. Ye, N. LaBarge, B.E. Logan, Performance of anaerobic fluidized membrane bioreactors using effluents of microbial fuel cells treating domestic wastewater, Bioresour. Technol. 208 (2016) 58–63.
[30] L. Ren, Y. Ahn, B.E. Logan, A two-stage microbial fuel cell and anaerobic fluidized bed membrane bioreactor (MFC-AFMBR) system for effective domestic wastewater treatment, Environ. Sci. Technol. 48 (7) (2014) 4199–4206.
[31] S.R. Dash, P. Bose, D. Ko, C. Lee, J. Kim, Integrating electrochemically-assisted anaerobic reactors with conductive media for enhanced methanation of greywater, Chem. Eng. J. 493 (2024) 152700.
[32] M. Chen, Y. Li, X. Sun, R. Dai, J. Zheng, X. Wang, Z. Wang, Recent advances in electrochemical processes integrated with anaerobic membrane bioreactor in wastewater treatment, Chem. Eng. J. 468 (2023) 143822.
[33] A. Ding, Q. Fan, R. Cheng, G. Sun, M. Zhang, D. Wu, Impacts of applied voltage on microbial electrolysis cell-anaerobic membrane bioreactor (MEC-AnMBR) and its membrane fouling mitigation mechanism, Chem. Eng. J. 333 (2018) 630–635.
[34] K.P. Katuri, C.M. Werner, R.J. Jimenez-Sandoval, W. Chen, S. Jeon, B.E. Logan, Z. Lai, G.L. Amy, P.E. Saikaly, A novel anaerobic electrochemical membrane bioreactor (AnEMBR) with conductive hollow-fiber membrane for treatment of low-organic strength solutions, Environ. Sci. Technol. 48 (21) (2014) 12833–12841.
[35] W.C. Lipps, T.E. Baxter, E.B. Braun-Howland, A.P.H. Association, A.W.W. Association, Standard methods for the examination of water and wastewater, American public health association, 2023.
[36] B. Wyrwas, A. Zgoła-Grześkowiak, Continuous flow methylene blue active substances method for the determination of anionic surfactants in river water and biodegradation test samples, J. Surfactant Deterg. 17 (1) (2014) 191–198.
[37] J. Bae, C. Shin, E. Lee, J. Kim, P.L. McCarty, Anaerobic treatment of low-strength wastewater: a comparison between single and staged anaerobic fluidized bed membrane bioreactors, Bioresour. Technol. 165 (2014) 75–80.
[38] M. DuBois, K.A. Gilles, J.K. Hamilton, P.t. Rebers, F. Smith, Colorimetric method for determination of sugars and related substances, Anal. Chem. 28 (3) (1956) 350–356.
[39] B. Frolund, T. Griebe, P. Nielsen, Enzymatic activity in the activated-sludge floc matrix, Appl. Microbiol. Biotechnol. 43 (1995) 755–761.
[40] H. Choi, J. Kim, J. Park, C. Lee, Response of granular anammox process under mainstream conditions to continuous and transient organic loads, Chem. Eng. J. 464 (2023) 142681.
[41] T. Rognes, T. Flouri, B. Nichols, C. Quince, F. Mahé, VSEARCH: a versatile open source tool for metagenomics, PeerJ 4 (2016) e2584.
[42] J. Kim, H. Choi, C. Lee, Formation and characterization of conductive magnetite-embedded granules in upflow anaerobic sludge blanket reactor treating dairy wastewater, Bioresour. Technol. 345 (2022) 126492.
[43] J. Kim, J. Park, H. Choi, C. Lee, Performance and stability enhancement of methanogenic granular sludge process: feed pre-acidification and magnetite-embedded granule formation, Chem. Eng. J. 469 (2023) 143864.
[44] G. Zhen, Y. Pan, Y. Han, Y. Gao, S.I. Gadow, X. Zhu, L. Yang, X. Lu, Enhanced co-digestion of sewage sludge and food waste using novel electrochemical anaerobic membrane bioreactor (EC-AnMBR), Bioresour. Technol. 377 (2023) 128939.
[45] K. Bani-Melhem, E. Smith, Grey water treatment by a continuous process of an electrocoagulation unit and a submerged membrane bioreactor system, Chem. Eng. J. 198 (2012) 201–210.
[46] S.B. Pillai, N.V. Thombre, Coagulation, flocculation, and precipitation in water and used water purification, in: Handbook of Water and Used Water Purification, Springer, 2023, pp. 1–25.
[47] L.-C. Hua, C. Huang, Y.-C. Su, T.-N.-P. Nguyen, P.-C. Chen, Effects of electro-coagulation on fouling mitigation and sludge characteristics in a coagulation-assisted membrane bioreactor, J. Membr. Sci. 495 (2015) 29–36.
[48] W. Chen, P. Westerhoff, J.A. Leenheer, K. Booksh, Fluorescence excitation–emission matrix regional integration to quantify spectra for dissolved organic matter, Environ. Sci. Technol. 37 (24) (2003) 5701–5710.
[49] T. Lütke-Eversloh, C.N.S. Santos, G. Stephanopoulos, Perspectives of biotechnological production of L-tyrosine and its applications, Appl. Microbiol. Biotechnol. 77 (2007) 751–762.
[50] K. Groenen-Serrano, E. Weiss-Hortala, A. Savall, P. Spitéri, Role of hydroxyl radicals during the competitive electrooxidation of organic compounds on a boron-doped diamond anode, Electrocatalysis 4 (2013) 346–352.
[51] A.K. Mruthunjaya, A.A. Torriero, Mechanistic aspects of the electrochemical oxidation of aliphatic amines and aniline derivatives, Molecules 28 (2) (2023) 471.
[52] M.W. Hakami, A. Alkhudhiri, S. Al-Batty, M.-P. Zacharof, J. Maddy, N. Hilal, Ceramic microfiltration membranes in wastewater treatment: filtration behavior, fouling and prevention, Membranes 10 (9) (2020) 248.
[53] Y. Hu, J. Wang, J. Shi, Y. Yang, J. Ji, R. Chen, A review of electro-conductive membrane enabled electrochemical anaerobic membrane bioreactor process for low-carbon wastewater treatment, J. Environ. Chem. Eng. 12 (5) (2024) 113494.
[54] J. Wang, K. Wang, W. Li, H. Wang, Y. Wang, Enhancing bioelectrochemical processes in anaerobic membrane bioreactors for municipal wastewater treatment: a comprehensive review, Chem. Eng. J. 484 (2024) 149420.
[55] Y. Han, W. Li, Y. Gao, T. Cai, J. Wang, Z. Liu, J. Yin, X. Lu, G. Zhen, Biogas upgrading and membrane anti-fouling mechanisms in electrochemical anaerobic membrane bioreactor (EC-AnMBR): focusing on spatio-temporal distribution of metabolic functionality of microorganisms, Water Res. 256 (2024) 121557.
[56] C. Niu, Z. Zhang, T. Cai, Y. Pan, X. Lu, G. Zhen, Sludge bound-EPS solubilization enhance CH4 bioconversion and membrane fouling mitigation in electrochemical anaerobic membrane bioreactor: insights from continuous operation and interpretable machine learning algorithms, Water Res. 264 (2024) 122243.
[57] G. Zhou, Y. Zhou, G. Zhou, L. Lu, X. Wan, H. Shi, Assessment of a novel overflow-type electrochemical membrane bioreactor (EMBR) for wastewater treatment, energy recovery and membrane fouling mitigation, Bioresour. Technol. 196 (2015) 648–655.
[58] S. Li, C. Cheng, A. Thomas, Carbon-based microbial-fuel-cell electrodes: from conductive supports to active catalysts, Adv. Mater. 29 (8) (2017) 1602547.
[59] M.B. Asif, T. Maqbool, Z. Zhang, Electrochemical membrane bioreactors: state-of-the-art and future prospects, Sci. Total Environ. 741 (2020) 140233.
[60] B.R. Dhar, Y. Gao, H. Yeo, H.-S. Lee, Separation of competitive microorganisms using anaerobic membrane bioreactors as pretreatment to microbial electrochemical cells, Bioresour. Technol. 148 (2013) 208–214.
[61] S. Zheng, F. Liu, B. Wang, Y. Zhang, D.R. Lovley, Methanobacterium capable of direct interspecies electron transfer, Environ. Sci. Technol. 54 (23) (2020) 15347–15354.
[62] P. Batlle-Vilanova, S. Puig, R. Gonzalez-Olmos, A. Vilajeliu-Pons, M.D. Balaguer, J. Colprim, Deciphering the electron transfer mechanisms for biogas upgrading to biomethane within a mixed culture biocathode, RSC Adv. 5 (64) (2015) 52243–52251.
[63] Y. Choi, D. Kim, J. Cha, H. Choi, G. Baek, C. Lee, Enhancing energy recovery from expired rice wine via microbial electrolysis of supernatant and anaerobic digestion of concentrate after gravity settling, J. Environ. Chem. Eng. 12 (6) (2024) 114654.
[64] C. Lee, Engineering direct interspecies electron transfer for enhanced methanogenic performance, in: Renewable Energy Technologies for Energy Efficient Sustainable Development, 2022, pp. 23–59.
[65] W.B. Whitman, F. Rainey, P. Kämpfer, M. Trujillo, J. Chun, P. DeVos, B. Hedlund, S. Dedysh, Bergey's Manual of Systematics of archaea and bacteria, Wiley Online Library, 2015.
[66] L. Ramadan, R. Deeb, C. Sawaya, C. El Khoury, M. Wazne, M. Harb, Anaerobic membrane bioreactor-based treatment of poultry slaughterhouse wastewater: microbial community adaptation and antibiotic resistance gene profiles, Biochem. Eng. J. 192 (2023) 108847.
[67] Q. Wang, Y. Liang, P. Zhao, Q.X. Li, S. Guo, C. Chen, Potential and optimization of two-phase anaerobic digestion of oil refinery waste activated sludge and microbial community study, Sci. Rep. 6 (1) (2016) 38245.
[68] S. Zhang, J. Chang, C. Lin, Y. Pan, K. Cui, X. Zhang, P. Liang, X. Huang, Enhancement of methanogenesis via direct interspecies electron transfer between Geobacteraceae and Methanosaetaceae conducted by granular activated carbon, Bioresour. Technol. 245 (2017) 132–137.
[69] V.K. Yadav, S.H. Khan, N. Choudhary, V. Tirth, P. Kumar, R.K. Ravi, S. Modi, A. Khayal, M.P. Shah, P. Sharma, Nanobioremediation: a sustainable approach towards the degradation of sodium dodecyl sulfate in the environment and simulated conditions, J. Basic Microbiol. 62 (3–4) (2022) 348–360.
[70] G. Baek, J. Kim, S. Lee, C. Lee, Development of biocathode during repeated cycles of bioelectrochemical conversion of carbon dioxide to methane, Bioresour. Technol. 241 (2017) 1201–1207.
[71] R. Yoo, J. Kim, P.L. McCarty, J. Bae, Anaerobic treatment of municipal wastewater with a staged anaerobic fluidized membrane bioreactor (SAF-MBR) system, Bioresour. Technol. 120 (2012) 133–139.